

Ultrafast coherent dynamics in quantum wells for multisubband excitation in different density regimes

S. Arlt, U. Siegner, F. Morier-Genoud, and U. Keller

Swiss Federal Institute of Technology Zurich, Institute of Quantum Electronics, ETH Honggerberg HPT, CH-8093 Zurich, Switzerland

(Received 16 April 1998; revised manuscript received 8 July 1998)

We present an experimental study of the coherent dynamics in quantum wells for the simultaneous excitation of Lorentzian excitons below the band edge and structured exciton Fano continua corresponding to higher-order subband transitions. Spectrally resolved transient four-wave mixing (FWM) experiments with 100 fs pulses were performed on a 500 Å broad GaAs/Al_xGa_{1-x}As quantum well over a wide range of carrier densities. At lower carrier densities, the dephasing times of the different exciton transitions were determined from the width of the narrow resonances in the distinctly structured FWM spectra. These data demonstrate that the decay of the FWM signal from exciton Fano continua in the time-delay domain is not determined by dephasing at the lowest carrier densities. This is indicative of quantum interference which has its origin in many-body exciton-continuum coupling. At higher carrier densities, the FWM spectra are much less structured due to stronger dephasing, quantum interference effects lose their importance, and the structured exciton Fano continua show properties similar to unstructured continua without embedded exciton transitions.
[S0163-1829(98)00744-9]

I. INTRODUCTION

Semiconductor quantum wells and quantum wires can possess several electron and hole subbands, depending on the properties of the confinement potential. In interband optics, the subband structure leads to the observation of several excitonic Rydberg series, each one corresponding to an optically allowed transition between an electron and a hole subband. The exciton resonance corresponding to the energetically lowest $n=1$ electron and hole subbands is well separated from continuum transitions by its binding energy and, therefore, is a discrete transition. In contrast, higher-order excitons corresponding to electron and hole subbands with $n>1$ are embedded in continuum states of lower electron and hole subband pairs. For atomic systems, it has been shown that coupling between energetically degenerate discrete and continuum states results in Fano interference¹ if both types of states can be optically excited from a common ground state. Fano interference manifests itself in linear optics by an asymmetric absorption line shape, known as the Fano profile.¹

In semiconductors, Coulomb coupling between higher-order excitons and lower-order continuum states has theoretically been shown to result in Fano interference and in the formation of Fano resonances in quantum wells and wires.²⁻⁴ The exciton Fano resonance is a structured continuum, consisting of a higher-order exciton coupled to energetically degenerate continuum states by the bare Coulomb potential.³ These structured continua are the true eigenstates of one- and two-dimensional semiconductors above the band edge. Experimentally, Fano absorption profiles have been observed in quantum wells⁵ and in bulk semiconductors under magnetic field.^{6,7} The linear optical properties of these coupled exciton-continuum resonances are well understood.²⁻⁶

Much less is known about the coherent nonlinear optical properties of quantum wells for multisubband excitation in-

volving the lowest discrete exciton transition and exciton Fano continua. In this paper, we present a detailed experimental study of the coherent emission from a quantum well for multisubband excitation. Spectrally resolved transient four-wave mixing (FWM) experiments with 100 fs pulses were performed over a wide range of carrier densities. These experiments will shed light on the nonlinear optical properties of two-dimensional exciton Fano continua in quantum wells.

To the best of our knowledge, the coherent emission from exciton Fano continua has only been studied for one-dimensional magnetoexcitons in bulk GaAs.⁸ We note that the lowest Lorentzian exciton shows a distinctly different behavior in coherent nonlinear optical experiments under a strong magnetic field compared to the zero-field case.⁹ Therefore, it is not clear *a priori* how the properties of magnetoexciton Fano continua compare to the properties of exciton Fano continua in quantum wells at zero field.

Moreover, our experiments address the question how coupling between the lowest Lorentzian exciton and the structured exciton Fano continua in the nonlinear regime affects the coherent emission from a quantum well. The interaction between the lowest Lorentzian exciton and continuum transitions has been studied for the unstructured “flat” continuum of the lowest subband¹⁰⁻¹⁵ and for the magnetoexciton system¹⁶ but not for exciton Fano continua in quantum wells at zero magnetic field. We will point out the similarities and differences between the different exciton-continuum systems.

The paper is organized as follows. In Sec. II, we briefly discuss our experimental technique. The results of transient FWM experiments for multisubband excitation of a quantum well at intermediate carrier densities are presented in Sec. III. We determine the dephasing times of the different resonances from the width of the emission lines in the FWM spectra. Our data show that the decay of the FWM emission from quantum-well exciton Fano continua versus the time

delay between the excitation laser pulses is not due to dephasing at these densities. This effect is attributed to quantum interference between exciton and continuum states, which has its origin in many-body exciton-continuum coupling. Similar results and conclusions were obtained in Refs. 8 and 16 for magnetoexciton Fano continua, showing that this effect is of general importance for exciton Fano resonances in semiconductors. In Sec. IV, we will discuss the properties of the coherent emission from quantum wells for multisubband excitation at high carrier densities. We finally present our conclusions in Sec. V.

II. EXPERIMENT

Four-wave-mixing experiments were performed with bandwidth-limited 100 fs pulses from a Ti:sapphire laser in the standard two-beam configuration with collinearly polarized excitation pulses with wave vectors \mathbf{k}_1 and \mathbf{k}_2 . Both pulses had equal intensities. The excitation pulses are separated in time by a variable time delay τ , which is controlled by a stepper motor. The nonlinear interaction in the sample gives rise to a FWM signal emitted in the phase-matching direction $2\mathbf{k}_2 - \mathbf{k}_1$. We detect the FWM signal either spectrally integrated [$\propto \int |P^{(3)}(\omega, \tau)|^2 d\omega$, where $P^{(3)}(\omega, \tau)$ is the nonlinear polarization in third order] as a function of the time delay τ or spectrally resolved [$\propto |P^{(3)}(\omega, \tau)|^2$] at fixed time delays τ . The spectrally resolved FWM measurements as well as linear absorption experiments were performed with a monochromator and a charge-coupled device (CCD) array providing an overall spectral resolution of 0.1 meV.

Since the bandwidth of the 100 fs excitation pulses is about 15 meV full width at half maximum (FWHM), we have chosen a quantum-well sample with a large well width and small subband separations. This sample contains ten 500 Å broad GaAs/Al_{0.3}Ga_{0.7}As quantum wells. To allow for transmission experiments, the GaAs substrate of the sample was removed by wet-etching. All experiments were performed at the temperature $T=7$ K.

III. DENSITIES WELL BELOW THE MOTT DENSITY

A. Experimental results

Figure 1 shows the low-temperature linear absorption spectrum of the 500 Å broad GaAs/Al_{0.3}Ga_{0.7}As multiple quantum well. The spectrum comprises several exciton resonances which correspond to transitions between electron (e) and heavy-hole (hh) subbands with the same quantum number n , labeled as $e1$ -hh1, $e2$ -hh2, and $e3$ -hh3. The lowest light-hole (lh) exciton resonance, $e1$ -lh1, is found energetically below the $e1$ -hh1 exciton. This is because mechanical strain at low temperatures has shifted both the hh and the lh valence bands to lower energies where the shift of the lh band is larger¹⁷ and overcompensates the difference in quantization energies of the $e1$ -hh1 and $e1$ -lh1 excitons. The linear absorption spectrum also shows several exciton resonances with $n_{\text{electron}} \neq n_{\text{hole}}$, which have a finite oscillator strength in quantum wells with a finite barrier height if $|n_{\text{electron}} - n_{\text{hole}}|$ is an even number.¹⁸ The lowest exciton transitions $e1$ -hh1 and $e1$ -lh1 have symmetric Lorentzian

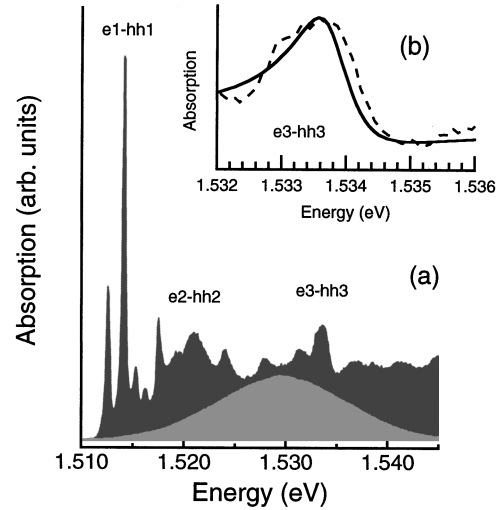


FIG. 1. (a) Linear absorption spectrum of the 500 Å GaAs/Al_{0.3}Ga_{0.7}As multiple quantum well (dark gray) and excitation laser spectrum (light gray) (temperature 7 K). (b) Close-up of the measured $e3$ -hh3 exciton absorption line shape (dashed line) and calculated Fano profile (solid line).

line shapes with a FWHM of only 0.4 meV, demonstrating small inhomogeneous and homogeneous broadening in this high-quality sample.

The higher-order exciton resonances are structured exciton Fano continua with an asymmetric line shape which is the signature of Fano interference between exciton transitions and energetically degenerate continuum transitions.¹ The different types of transitions are coupled by the bare Coulomb potential.³ If the exciton resonances are spaced from each other far enough so that the model of a single discrete resonance coupled to a continuum can be applied, the absorption line shape can be fitted by the expression $\alpha(\varepsilon) \propto (\varepsilon - q)^2 / (1 + \varepsilon^2)$ for the Fano absorption profile.¹ Additional homogeneous broadening is neglected.¹⁹ In this expression, ε is the photon energy shifted by the energy of the discrete state and normalized by the strength Γ of the coupling between the continuum and the discrete state. The parameter q essentially describes the ratio of the optical matrix elements between the ground state and the discrete state and between the ground state and the continuum states. We apply the above expression to the $e3$ -hh3 exciton resonance, which is fairly well separated from the adjacent resonances. Figure 1(b) shows a close-up of the measured absorption line shape of the $e3$ -hh3 resonance and the calculated Fano profile for the parameters $q = -2.41$ and $\Gamma = 0.53$ meV. A reasonable fit is obtained, which reconfirms the results of previous work.²⁻⁵

In the FWM experiments, the excitation laser spectrum, centered at 1.530 eV, is tuned slightly below the $e3$ -hh3 resonance to excite simultaneously the lowest $e1$ -lh1 and $e1$ -hh1 excitons and higher-order exciton Fano continua, as shown in Fig. 1. Power spectra of the FWM signal are plotted in Fig. 2 for different time delays τ between -100 and 167 fs and a carrier density $N_0 \approx 3 \times 10^{10}$ cm⁻² per excitation pulse. Unlike the excitation pulse spectrum, the FWM spectra show a distinct structure which arises from the exciton transitions which are embedded in the continuum. This

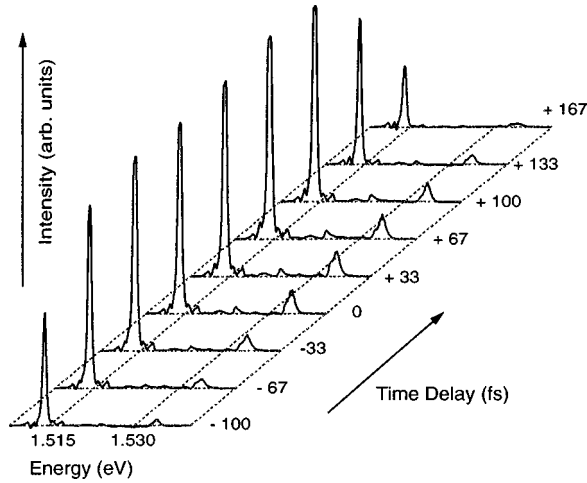


FIG. 2. Power spectrum of the four-wave-mixing signal for multisubband excitation for different time delays. Carrier density $N_0 \approx 3 \times 10^{10} \text{ cm}^{-2}$, temperature 7 K.

distinct structure is the signature of multisubband excitation at lower densities. The largest emission line in the FWM spectrum at 1.514 eV originates from the $e1\text{-hh1}$ exciton. A significant contribution to the FWM spectrum at 1.534 eV can be traced back to the $e3\text{-hh3}$ exciton Fano continuum. Very small contributions from the $e2\text{-hh2}$ transition and from transitions with $n_{\text{electron}} \neq n_{\text{hole}}$ are also visible. All emission lines in the FWM spectrum are much narrower than the laser spectrum. Since the dominating $e1\text{-hh1}$ and $e3\text{-hh3}$ resonances are well separated from the adjacent resonances, these FWM resonances can be analyzed more quantitatively.

In Fig. 3, we have plotted the FWHM of the $e1\text{-hh1}$ Lorentzian resonance and the $e3\text{-hh3}$ Fano resonance versus time delay for the excitation density $N_0 \approx 3 \times 10^{10} \text{ cm}^{-2}$ (open symbols), as obtained from Fig. 2. The filled symbols mark the FWHM of the resonances at the increased carrier density $3N_0$ and the dashed line is the width of the $e1\text{-hh1}$

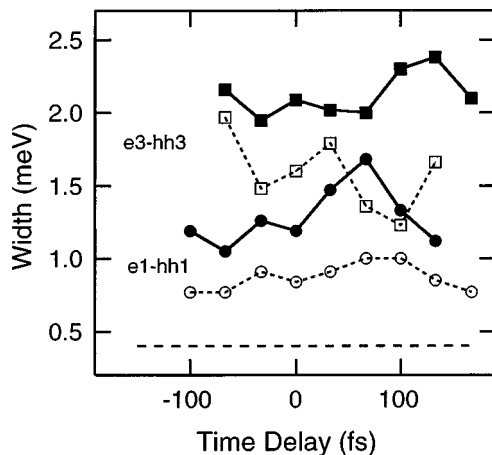


FIG. 3. Full width at half maximum of the resonances in the four-wave-mixing spectra. Dots, $e1\text{-hh1}$ exciton; squares, $e3\text{-hh3}$ exciton Fano continuum. Open symbols, carrier density $N_0 \approx 3 \times 10^{10} \text{ cm}^{-2}$; filled symbols, density $3N_0$ (temperature 7 K). Dashed line, full width at half maximum of the $e1\text{-hh1}$ exciton resonances in the low-temperature linear absorption spectrum.

resonance in the linear absorption spectrum in Fig. 1, i.e., at zero carrier density. We note that the FWHM of both resonances is essentially independent of the time delay but increases with increasing excitation density. The density dependence of the linewidth of the $e1\text{-hh1}$ resonance in the density range between zero and $3N_0$ demonstrates that density-independent inhomogeneous broadening makes only a small contribution to the linewidth for densities of N_0 and larger in this high-quality sample. The measured linewidths for N_0 and $3N_0$ are dominated by homogeneous broadening, which is enhanced at higher carrier densities due to increased carrier-carrier scattering. Two features of the data are noteworthy. (i) For a fixed carrier density, the homogeneous linewidth of the $e3\text{-hh3}$ exciton Fano resonance is always larger than the homogeneous linewidth of the $e1\text{-hh1}$ Lorentzian exciton. From Fig. 3, we obtain average linewidths of 0.87 and 1.58 meV for N_0 , and 1.29 and 2.13 meV for $3N_0$, respectively. This result reflects that, for Fano resonances, the coupling Γ to the energetically degenerate continuum is an additional intrinsic contribution to the total homogeneous broadening, which adds to the natural homogeneous broadening γ resulting from quasiparticle scattering.¹⁹ (ii) The Fano coupling Γ is expected to decrease with increasing carrier density¹⁹ because Γ is due to Coulomb interaction,³ which is weakened by screening at elevated carrier densities. However, we observe that the total homogeneous linewidth of the $e3\text{-hh3}$ exciton Fano resonance increases with increasing carrier density. Consequently, we conclude that the natural homogeneous broadening γ shows a strong increase with increasing carrier density which overcompensates the decrease of the Fano coupling Γ . The same conclusion as for exciton Fano continua in quantum wells was reached for Fano magnetoexcitons.¹⁹

Since inhomogeneous broadening is negligible at the carrier densities N_0 and $3N_0$, we can estimate the dephasing times of the different resonances from the FWHM of the emission lines in the FWM spectrum. A single dephasing time characterizes each resonance for a given carrier density since the FWHM of the resonances does not show a significant dependence on the time delay. We use the fundamental relation $t_D = T_2/2 = \hbar/\delta E$, where t_D is the decay time, T_2 is the dephasing time, and δE is the FWHM of the emission lines.¹⁶ From this relation and from the average FWHM, we can estimate dephasing times of 1.5 and 1.0 ps for the $e1\text{-hh1}$ exciton at the excitation density N_0 and $3N_0$, respectively. For the $e3\text{-hh3}$ resonance, we obtain dephasing times of 0.83 ps at N_0 and 0.61 ps at $3N_0$. We note that LO-phonon emission does not limit the dephasing time of the $e3\text{-hh3}$ transition since the small subband separations in the 500 Å quantum well prohibit this process.

Figure 4 shows the spectrally integrated FWM signals for multisubband excitation and carrier densities N_0 and $3N_0$. The spectrally integrated FWM signals as a function of the time delay between the excitation pulses follow the excitation laser pulse shape over almost two orders of magnitude, i.e., the signals decay with a time constant of less than 100 fs. Importantly, for the excitation density N_0 none of the exciton resonances has a shorter dephasing time than the $e3\text{-hh3}$ exciton. This dephasing time is 0.83 ps, much longer than the pulse-width limited decay of the spectrally integrated FWM signal in the time-delay domain. Consequently,

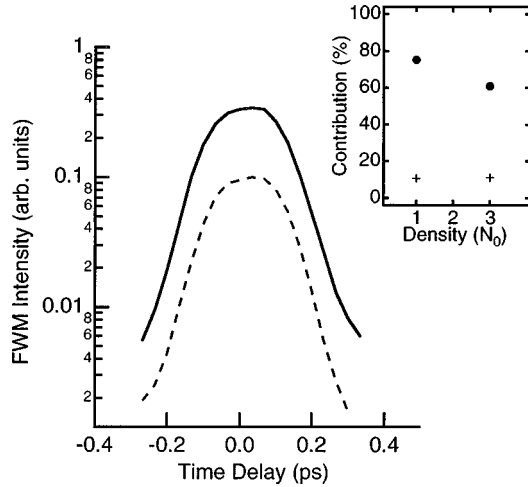


FIG. 4. Spectrally integrated four-wave-mixing signal vs time delay for multisubband excitation. Dashed line, carrier density $N_0 \approx 3 \times 10^{10} \text{ cm}^{-2}$; solid line, carrier density $3N_0$ (temperature 7 K). Inset, relative contribution of the $e1-hh1$ (dots) and $e3-hh3$ (crosses) transitions to the total four-wave-mixing emission vs carrier density.

we conclude that the pulse-width limited decay of the spectrally integrated FWM signal is not caused by dephasing for multisubband excitation at the lowest density N_0 . For the density $3N_0$, dephasing is faster and the difference between the dephasing times and the decay time of the spectrally integrated FWM signal becomes smaller.

In the inset of Fig. 4, we have plotted the relative contribution of the different resonances to the total FWM emission versus carrier density. We will discuss in more detail in Sec. IV that this relative contribution shows no significant dependence on the time delay in the parameter range investigated here. Therefore, the average over the time delay could be plotted in the inset of Fig. 4. The coherent emission from the Lorentzian $e1-hh1$ exciton (dots) is at least 60% of the total FWM emission for the excitation densities N_0 and $3N_0$. The contribution from the $e3-hh3$ resonance (crosses) is about 10% of the total FWM emission at these densities. Therefore, the pronounced pulse-width limited decay of the total, spectrally integrated FWM signal versus time delay implies that neither the coherent emission from the $e1-hh1$ exciton nor the coherent emission from the $e3-hh3$ exciton Fano continuum shows a pronounced slowly decaying tail which would reflect the dephasing time of the respective resonances. For multisubband excitation at the lowest density N_0 , the coherent emission from both the $e1-hh1$ and the $e3-hh3$ resonances decays much faster in the time-delay domain than predicted by the dephasing times of the respective transitions. Consequently, the decay of the coherent emission from the $e1-hh1$ exciton and from the $e3-hh3$ Fano continuum in the time-delay domain is not due to dephasing for multisubband excitation at the density N_0 .

In contrast, the decay of the coherent emission from the $e1-hh1$ exciton versus time delay reflects the dephasing time if only the Lorentzian excitons at the band edge are excited (data not shown), as expected.²⁰ We conclude that the simultaneous excitation of the Lorentzian exciton is not the reason for the discrepancy between the decay in the time-delay domain and the time scale of dephasing observed for the

$e3-hh3$ exciton Fano continuum. This discrepancy is an inherent property of exciton Fano continua in quantum wells.

These findings for exciton Fano continua in quantum wells are attributed to quantum interference between exciton and continuum transitions. We refer to this effect as destructive quantum interference. Destructive quantum interference manifests itself by a pulse-width limited decay of the FWM signal in the time-delay domain if the dephasing time of the resonance is much longer than the pulse width. The pulse-width limited decay dominates the shape of the FWM signal in the time-delay domain and any slowly decaying contribution to the signal is much smaller than expected from the weight of the slowly dephasing resonance in the FWM spectrum.

The same behavior as for exciton Fano continua in quantum wells at zero magnetic field was found for magnetoexciton Fano continua.^{8,16} This shows that destructive quantum interference is of general importance for exciton Fano continua in one- and two-dimensional semiconductors, regardless of the application of a magnetic field.

The coherent emission from the Lorentzian exciton is also affected by destructive quantum interference in the multisubband experiments at the density N_0 in which exciton Fano continua are excited. A pulse-width limited decay in the time-delay domain is observed although the dephasing time of the Lorentzian exciton is much longer than the pulse width. Similar results were obtained at low densities for the simultaneous excitation of the exciton and an energetically separated broadband flat continuum of the same subband¹²⁻¹⁵ and for the interaction between Fano magnetoexciton continua and Lorentzian magnetoexcitons.¹⁶ This comparison shows that the discrepancy between the decay in the time-delay domain and the time scale of dephasing of the lowest exciton is of general importance in exciton-continuum systems, irrespective of the properties of the continuum. As a consequence, destructive quantum interference dominates the decay of the FWM emission in the time-delay domain for multisubband excitation in quantum wells at low and intermediate densities.

B. Discussion

With regard to the mechanism of destructive quantum interference, we first note that the effect for a single Fano continuum cannot be explained in the framework of the atomic physics Fano model¹ even though this model can be used to describe the linear absorption line shape, as shown in Fig. 1. For a single Fano continuum, the atomic physics Fano model predicts a decay of the FWM emission in the time-delay domain which is determined by the dephasing time,¹⁶ in disagreement with the experimental result. The discrepancy between the fast decay of the FWM signal in the time-delay domain and the dephasing time can only be understood if many-body Coulomb effects are considered both for a single exciton Fano continuum and for the excitation of the lowest exciton and an energetically separated continuum.^{8,12,13,15,16}

To further illustrate this point for a single exciton Fano continuum, we recall that the atomic physics Fano model¹ can be transformed into a system consisting of a ground state optically coupled to N excited states where the line shape of

the resonance is reflected by the energy dependence of the optical matrix element between the ground and the excited states.^{1,21} In such an N -level system, the dynamics of the coherent emission is the same in the real time and the time-delay domain for short-pulse excitation.²¹ Consequently, a pulse-width limited decay of the spectrally integrated FWM signal versus time delay implies a pulse-width limited decay of the coherent emission in real time. Due to the Fourier relation between energy and real time, this simple model predicts a FWM spectrum which is as broad as the excitation laser spectrum in this situation, in disagreement with the experimental data.

An obvious shortcoming of the above model is the assumption of a constant coupling strength between discrete and continuum transitions. In semiconductors, the intersubband coupling results from Coulomb interaction,³ which is weakened by screening with increasing carrier density. In fact, for magnetoexciton Fano continua it has been experimentally observed that the Fano coupling Γ decreases with increasing carrier densities.¹⁹ Therefore, the assumption of constant Fano coupling is only justified for linear absorption experiments where indeed the absorption profiles of exciton Fano continua in quantum wells and in bulk semiconductors under magnetic field can be described by the expressions of the atomic physics Fano model.^{5,6} Besides the weakening of the Fano coupling Γ , the natural homogeneous broadening γ of exciton Fano continua strongly increases with increasing carrier density in nonlinear optical experiments due to carrier-carrier scattering. This has been shown for exciton Fano continua in quantum wells by the analysis of the experimental data in Fig. 3 and has also been observed for magnetoexciton Fano continua.¹⁹ The density dependence of the homogeneous broadening of exciton Fano continua suggests to consider excitation-induced dephasing (EID).²² Excitation-induced dephasing results from screening of the Coulomb interaction in nonlinear optical experiments and manifests itself by a density-dependent dephasing rate.²²

EID has been considered in order to model FWM experiments where only the lowest exciton at the band edge and an energetically separated broadband continuum of the lowest subband were excited.¹²⁻¹⁵ In such single-subband experiments at low densities, a pulse-width limited decay of the FWM emission in the time-delay domain was observed.¹²⁻¹⁴ The corresponding FWM spectrum showed only a narrow line at the spectral position of the exciton from which a dephasing time much longer than the pulse width could be deduced.¹²⁻¹⁴ These experimental results were modeled introducing a density-dependent dephasing rate in the semiconductor Bloch equations.¹³⁻¹⁵ As a consequence, the carrier population in the continuum states can modify the polarization of the exciton.¹³⁻¹⁵ This is the essence of the nonlinear exciton-continuum coupling. It has also been pointed out that the coupling between exciton and continuum states due to EID can be described by a common ground-state picture in which quantum interference effects naturally occur.¹²

Further theoretical studies including EID on a phenomenological level have shown that the FWM spectrum consists of a spectrally narrow line at the discontinuity of the linear absorption spectrum.¹⁵ Therefore, for the excitation of structured exciton Fano continua, it is expected that the FWM spectrum comprises narrow emission lines corresponding to

the exciton Fano resonances. The decay of the FWM signal in the time-delay domain is expected to follow the excitation pulse.¹⁵ Our experimental observations in Figs. 2 and 4 are in agreement with the EID model. These results suggest to attribute the destructive quantum interference effect observed for exciton Fano continua in quantum wells and in bulk semiconductors under magnetic field^{8,16} to the many-body exciton-continuum coupling resulting from EID. In this regard, it is important to distinguish between the effects of the many-body exciton-continuum coupling and the exciton-continuum coupling due to the bare Coulomb potential at zero carrier density. While the former results in destructive quantum interference in nonlinear optical experiments, the latter gives rise to Fano interference observed in linear optical-absorption spectra.

Of course, the dynamics of the lowest Lorentzian exciton when excited together with exciton Fano continua in multi-subband excitation experiments can also be described by the EID model since this experimental situation closely resembles the single-subband experiments in Refs. 12–15.

The theory discussed so far is purely phenomenological. A more rigorous theory for the nonlinear optical properties of exciton Fano continua in semiconductors has to treat many-body Coulomb effects on a microscopic level in order to pinpoint the mechanisms responsible for exciton-continuum coupling in the nonlinear regime and destructive quantum interference. We are not aware of a microscopic many-body theory which addresses this problem. Such a theory is highly desirable in view of the increased importance of broadband ultrafast pulse excitation in nonlinear optics of semiconductors.

IV. HIGH-DENSITY REGIME

The studies of the nonlinear optical coherent response of the 500 Å quantum well were extended to the carrier density $10N_0 \approx 3 \times 10^{11} \text{ cm}^{-2}$. This density is approximately equal to the Mott density calculated for GaAs quantum wells with infinitely high barriers.²³ Power spectra of the FWM emission at this density are plotted in Fig. 5 for time delays between -33 fs (bottom) and 167 fs (top). The spectra show contributions from the Lorentzian $e1\text{-hh1}$ and $e1\text{-lh1}$ excitons below 1.517 eV , from the $e2\text{-hh2}$ and $e3\text{-hh3}$ Fano continua at 1.521 and 1.534 eV , respectively, as well as from transitions with $n_{\text{electron}} \neq n_{\text{hole}}$. Compared to the data for the density N_0 in Fig. 2, all emission lines are much broader and the FWM spectra are much less structured. Moreover, the shape of the high-density FWM spectra significantly depends on the time delay, in contrast to the results for the density N_0 . The data in Fig. 5 show that the Lorentzian excitons below the band edge contribute less to the total FWM emission at the largest positive time delay $\tau = 167 \text{ fs}$ than at earlier time delays. The spectrally integrated FWM signal as a function of the time delay is pulse-width limited for the density $10N_0$ (data not shown), as for lower densities.

A more quantitative analysis of the FWM spectra is presented in Fig. 6, where the relative contributions of the $e1\text{-hh1}$ and the $e3\text{-hh3}$ transitions are plotted versus time delay for carrier densities N_0 (circles), $3N_0$ (triangles), and $10N_0$ (squares). We define the relative contribution of a resonance as the area of the resonance in the FWM spectrum

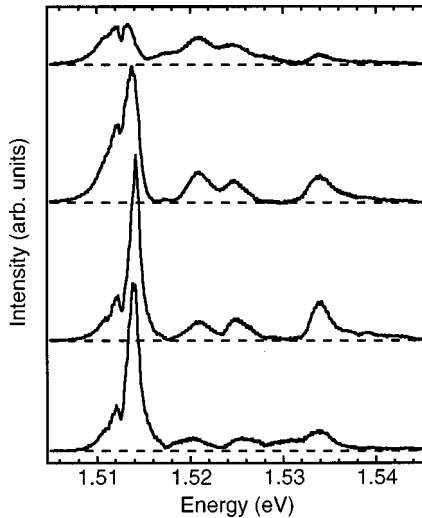


FIG. 5. Power spectrum of the four-wave-mixing signal for multisubband excitation for time delays -33 , $+33$, $+100$, and $+167$ fs (from bottom to top). Carrier density $10N_0 \approx 3 \times 10^{11} \text{ cm}^{-2}$, temperature 7 K.

divided by the total area of the spectrum. The relative contribution of the different resonances does not significantly depend on the time delay for the densities N_0 and $3N_0$, as already mentioned in Sec. III. At the highest density $10N_0$, the $e1$ -hh1 resonance loses strength at large time delays, as discussed for Fig. 5. This is not reflected in Fig. 6 because a quantitative analysis of the $e1$ -hh1 resonance was not performed at large time delays since it seemed too uncertain due to the increased spectral overlap of the broadened emission lines. For the same reason, we did not attempt a quantitative analysis of the $e3$ -hh3 emission line at $10N_0$. However, the data in Fig. 6 clearly demonstrate that the relative contribution of the Lorentzian $e1$ -hh1 exciton drops from 75% to 60% and below 50% with increasing carrier density for a fixed time delay. The relative contribution of the $e3$ -hh3 Fano continuum stays constant at about 10% at N_0 and $3N_0$. The decrease of the $e1$ -hh1 contribution for a constant $e3$ -hh3 contribution implies that the contributions from the $e2$ -hh2 Fano continuum and from transitions with $n_{\text{electron}} \neq n_{\text{hole}}$ are enhanced as the carrier density increases.

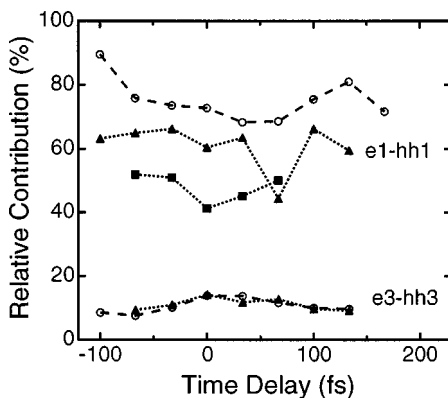


FIG. 6. Relative contribution of the $e1$ -hh1 (upper half) and the $e3$ -hh3 (lower half) transitions to the total four-wave-mixing emission vs time delay for carrier densities $N_0 \approx 3 \times 10^{10} \text{ cm}^{-2}$ (circles), $3N_0$ (triangles), and $10N_0$ (squares), temperature 7 K.

With regard to the shape of the high-density FWM spectra, we recall that the natural homogeneous broadening γ of exciton Fano resonances strongly increases with increasing density due to dephasing resulting from carrier-carrier scattering. Likewise, screening at higher carrier densities weakens the Coulomb Fano coupling. This has been directly experimentally observed for magnetoexciton Fano continua.¹⁹ Both effects result in a loss of the structure of the Fano absorption spectrum which smears out and broadens with increasing density.¹⁹ The same effect is seen in the high-density FWM spectra in Fig. 5, which do not show the distinct structure of the FWM spectra at the density N_0 due to the increased homogeneous broadening.

As an important consequence of the strong dephasing at high densities, there is not a clear discrepancy anymore between the pulse-width limited dynamics in the time-delay domain and the width of the FWM spectrum or the dephasing times. Therefore, quantum interference effects become less important at higher carrier densities and the dynamics is dominated by the strong dephasing.

With respect to the data in Fig. 6, we note that the contribution from the Lorentzian $e1$ -hh1 exciton to the FWM emission is rather large, given the small overlap of the laser spectrum with this resonance. This is at least partially due to the large oscillator strength of the lowest exciton as compared to the exciton Fano continua.¹¹ This excitonic enhancement of the lowest exciton²⁴ is already seen in the linear absorption spectrum. The nonlinear exciton-continuum coupling^{10,15,25} and the longer dephasing time²⁶ may also contribute to the intense FWM emission at the spectral position of the lowest exciton. The data in Fig. 6 indicate that the excitonic enhancement of the lowest exciton is reduced as the carrier density approaches the Mott density. This reflects the reduction of the oscillator strength of the lowest exciton due to the decrease of the binding energy.¹¹ This mechanism is not equally effective for higher-order exciton Fano resonances, which shows the continuum nature of these transitions. In fact, the same relative decrease of the FWM contribution from the lowest exciton and the increase of the continuum contribution with increasing density have been observed in single-subband experiments on the lowest exciton and a flat continuum.¹¹ Therefore, for higher carrier densities, flat continua and structured exciton Fano continua behave similarly in this respect.

For multisubband excitation, the time-delay dependence of the shape of the FWM spectrum is only observed at the highest density. The relative decrease of the coherent emission from the lowest exciton at positive time delays is reminiscent of the results for single-subband excitation of the lowest exciton and a flat continuum.^{10,25,27} The comparison between the single-subband and multisubband excitation results indicates that, at high carrier densities, the exciton Fano continua show a behavior similar to a flat continuum.

Summarizing these findings, we can state that the distinct structure of the FWM spectra, which is the signature of multisubband excitation at lower densities, is washed out at high carrier densities. With increasing density, the FWM spectra for multisubband excitation resemble more and more the spectra obtained for single-subband excitation of the lowest exciton and a flat continuum. Moreover, at high densities, the FWM spectra for multisubband and single-subband excita-

tion show similar features with respect to their time-delay dependence and with respect to the density dependence of the contributions from the lowest exciton and the continuum transitions. These findings are reasonable in view of the increased dephasing. Due to this strong dephasing at high carrier densities, quantum interference effects lose their importance.

V. CONCLUSIONS

We have presented a comprehensive experimental study of the linear absorption and the nonlinear optical coherent response of a quantum well for multisubband excitation. The lowest Lorentzian exciton below the band edge and exciton Fano continua corresponding to higher-order subband transitions are simultaneously excited in multisubband excitation experiments. Fano interference between energetically degenerate exciton and continuum transitions is clearly observed in the linear absorption spectrum at zero carrier density, which reconfirms the results of previous work.⁵ Fano interference in linear absorption spectra and the formation of the coupled exciton-continuum state are well understood considering coupling between different subbands which results from the bare unscreened Coulomb potential at zero density.³

The FWM experiments at carrier densities well below the Mott density demonstrate that the signature of multisubband excitation is a distinctly structured FWM power spectrum. The FWM spectrum comprises narrow emission lines, which can be traced back to the Lorentzian exciton and the exciton Fano continuum transitions. The negligible inhomogeneous broadening in our high-quality sample has allowed us to estimate the dephasing times of the different resonances from the width of the FWM emission lines. The analysis has clearly demonstrated that the decay of the FWM emission from exciton Fano continua in the time-delay domain is not caused by dephasing at lower carrier densities. This particular dynamics is attributed to destructive quantum interference

between exciton and continuum transitions resulting from many-body exciton-continuum coupling. We have discussed that many-body exciton-continuum coupling can result from excitation-induced dephasing, following the lines of earlier work on the exciton and an energetically separated continuum.¹²⁻¹⁵ The effect of many-body exciton-continuum coupling is to be distinguished from the effect of the exciton-continuum coupling by the bare Coulomb potential which results in Fano interference seen in linear spectra. Since the same dynamics as for exciton Fano continua in quantum wells at zero magnetic field was observed for magnetoexciton Fano continua in bulk GaAs,^{8,16} we conclude that destructive quantum interference is of general importance for exciton Fano continua in low-dimensional semiconductors, irrespective of the type of the quantum confinement.

In the FWM experiments at a higher carrier density approximately equal to the Mott density, we observe broad FWM spectra with a continuum contribution which is much less structured than at lower densities. At high carrier densities, the exciton Fano continua show a behavior similar to flat continua. Quantum interference effects lose their importance due to the strong dephasing.

In conclusion, we have demonstrated that the coupling between excitons and energetically degenerate continuum transitions considerably affects the optical properties of semiconductor quantum wells for multisubband excitation. Depending on the carrier density, Fano interference, destructive quantum interference, or dephasing-dominated dynamics are observed.

ACKNOWLEDGMENTS

We would like to acknowledge helpful discussions with D. S. Chemla and P. Thomas. This work has been supported by the Swiss National Science Foundation under Contract No. 21-49298.96.

¹U. Fano, *Phys. Rev.* **124**, 1866 (1961).

²A. R. K. Willcox and D. M. Whittaker, *Superlattices Microstruct.* **16**, 59 (1994).

³S. Glutsch, D. S. Chemla, and F. Bechstedt, *Phys. Rev. B* **51**, 16 885 (1995).

⁴R. Winkler, *Phys. Rev. B* **51**, 14 395 (1995).

⁵D. Y. Oberli, G. Böhm, G. Weimann, and J. A. Brum, *Phys. Rev. B* **49**, 5757 (1994).

⁶S. Glutsch, U. Siegner, M.-A. Mycek, and D. S. Chemla, *Phys. Rev. B* **50**, 17 009 (1994).

⁷T. Hornung and R. G. Ulbrich, *Physica B & C* **117B&118B**, 263 (1983).

⁸U. Siegner, M.-A. Mycek, S. Glutsch, and D. S. Chemla, *Phys. Rev. Lett.* **74**, 470 (1995).

⁹P. Kner, S. Bar-Ad, M. V. Marquezini, D. S. Chemla, and W. Schäfer, *Phys. Rev. Lett.* **78**, 1319 (1997).

¹⁰T. Rappen, U. Peter, M. Wegener, and W. Schäfer, *Phys. Rev. B* **48**, 4879 (1993).

¹¹A. Lohner, K. Rick, P. Leisching, A. Leitenstorfer, T. Elsässer, T. Kuhn, F. Rossi, and W. Stolz, *Phys. Rev. Lett.* **71**, 77 (1993).

¹²S. T. Cundiff, M. Koch, W. H. Knox, J. Shah, and W. Stolz, *Phys. Rev. Lett.* **77**, 1107 (1996).

¹³M. U. Wehner, D. Steinbach, and M. Wegener, *Phys. Rev. B* **54**, R5211 (1996).

¹⁴D. Birkedal, V. G. Lyssenko, J. M. Hvam, and K. El Sayed, *Phys. Rev. B* **54**, 14 250 (1996).

¹⁵K. El Sayed, D. Birkedal, V. G. Lyssenko, and J. M. Hvam, *Phys. Rev. B* **55**, 2456 (1997).

¹⁶U. Siegner, M.-A. Mycek, S. Glutsch, and D. S. Chemla, *Phys. Rev. B* **51**, 4953 (1995).

¹⁷F. H. Pollak and M. Cardona, *Phys. Rev.* **172**, 816 (1968).

¹⁸C. Weisbuch and B. Vinter, *Quantum Semiconductor Structures: Fundamentals and Applications* (Academic, San Diego, 1991).

¹⁹M. V. Marquezini, P. Kner, S. Bar-Ad, J. Tignon, and D. S. Chemla, *Phys. Rev. B* **57**, 3745 (1998).

²⁰J. Shah, *Ultrafast Spectroscopy of Semiconductors and Semiconductor Nanostructures* (Springer-Verlag, Berlin, 1996).

²¹T. Meier, A. Schulze, P. Thomas, H. Vaupel, and K. Maschke, *Phys. Rev. B* **51**, 13 977 (1995).

²²H. Wang, K. Ferrio, D. G. Steel, Y. Z. Hu, R. Binder, and

- S. W. Koch, Phys. Rev. Lett. **71**, 1261 (1993).
- ²³S. Nojima, Phys. Rev. B **51**, 11 124 (1995).
- ²⁴R. G. Ulbrich, in *Optical Nonlinearities and Instabilities in Semiconductors*, edited by H. Haug (Academic, New York, 1988).
- ²⁵T. Rappen, U.-G. Peter, M. Wegener, and W. Schäfer, Phys. Rev. B **49**, 10 774 (1994).
- ²⁶D.-S. Kim, J. Shah, J. E. Cunningham, T. C. Damen, W. Schäfer, M. Hartman, and S. Schmitt-Rink, Phys. Rev. Lett. **68**, 1006 (1992).
- ²⁷A. Leitenstorfer, A. Lohner, K. Rick, P. Leisching, T. Elsässer, T. Kuhn, F. Rossi, W. Stolz, and K. Ploog, Phys. Rev. B **49**, 16 372 (1994).